MDPI

Article

General Trends in the Compression of Glasses and Liquids

Oliver Tschauner [ID]

Department of Geoscience, University of Nevada Las Vegas, Las Vegas, NV 89154, USA; oliver.tschauner@unlv.edu

Abstract: The present work relates the isothermal volumes of silicate glasses and melts to the combined ionic volumes of their chemical constituents. The relation is an extension of a relation that has already been established for crystalline oxides, silicates, alumosilicates, and other materials that have O^{2-} as a constituent anion. The relation provides constraints on bond coordination, indicates pressure-induced changes in coordination in melts and glasses and interatomic distances, and quantifies the extent of transitory regions in pressure-induced coordination changes.

Keywords: glasses; melts; coordination change; amorphous transitions; transitory structures; isotherms

1. Introduction

Examining the compression of amorphous materials in general and of liquids in particular over pressures in the range of 10 to 100 GPa poses particular experimental and theoretical challenges. Whereas the assessment of density in compression studies of crystalline phases is, at least conceptually, rather straightforward through the use of Bragg diffraction and crystal structure analysis, the analysis of elastic X-ray scattering of amorphous materials is much more difficult and alternative approaches that are based on inelastic scattering techniques, X-ray attenuation, refractive index, and sink–float experiments come with their own challenges [1–10]. Moreover, experimental studies of the compression of silicate melts have to cope with technical difficulties that arise from the combination of both high pressure and high temperature.

In a recent paper [11], it was shown for a large number of solids that their observed volumes scale linearly with their ionic volumes as function of pressure within narrow uncertainties. Upon the compression of solids, differences in bond strength and electron density along different crystallographic directions and for atoms on different sites are sufficiently well averaged to give rise to this linear relation. The post-Hookean compression of oxides and halogenides that causes the pressure-dependence of their bulk moduli is controlled by the non-linear anion crystal radii contraction and, thus, by the type of the anion, its coordination, and by stoichiometry. The influence of structure-specific sterical and geometric parameters enters through the linear coefficients that relate molar and ionic volumes because they are similar for isotypic phases [11]. The solids examined in [11] include framework materials as well as compact high-pressure phases, oxides, silicates, borates, alumo- and beryllosilicates, complex salts, halides, and metalorganic frameworks.

The correlation of molar and ionic volume compression in [11] also serves as an independent test of the validity of the pressure-dependent crystal radii that have been derived in [12].

The observations in [11] suggest that an equivalent correlation holds for amorphous materials. The present paper examines the correlation between molar and ionic volumes of glasses and melts with O^{2-} as the constituent anion as function of pressure. In particular, it is examined (a) if this correlation detects amorphous–amorphous transitions, notably coordination and valence changes in amorphous materials, (b) if one can assess bond coordination through this correlation, and (c) if it can be used to assess the width of the pressure range of transitory states of structural transitions in amorphous materials.

The answer to this latter question also addresses a more fundamental problem: coordination changes in amorphous condensed matter may in general be gradual and extend over vast ranges of pressure–temperature (P-T). In such cases the concept of an equation of state is formally invalid because the latter is a measure of changes in the state of a phase under varying parameters, such as P and T, under the assumption of reversible paths and a well-defined groundstate at reference conditions. This condition is not necessarily given if the bond coordination of the constituting elements in the material changes along with P and T and is thus not always reversible (in fact, in many cases it is not, e.g., in [13]). For such materials, compression needs to be represented as a function of changing groundstate as well as changing P and T. The approach of the present work may allow for examining the extent of such intermediate regions and whether they dominate the behavior of amorphous materials over extended ranges of compression or within a narrow compression range only. Overall, this paper aims to provide a tool for the analysis of compression data of amorphous materials.

2. Materials and Methods

The present study is constrained to glasses and liquids that have O^{2-} as a constituent anion. The approach is based on the recent observation that the molar volumes of solids with O^{2-} as a constituent anion are generally in a linear relation to their ionic volumes [11]. The ionic volumes are defined as

$$V_{ion} = \frac{4\pi}{3} \cdot \left[i \cdot r_A^3 + j \cdot r_B^3 + k \cdot r_C^3 + \cdots \right] \tag{1}$$

for a compound $A_iB_jC_k\ldots$ where i, j, k,... give the stoichiometry of the chemical species A, B, C,... and the radii r_A, r_B, r_C,... are the crystal radii for a given valence and bond coordination [14]. The pressure-dependences of crystal radii for a large number of chemical species, valence, and spin states have been reported in [12]. With this definition of the ionic volume, there is a linear relation

$$V_{mol}(P) = A \cdot V_{ion}(P) - V' \tag{2}$$

between the ionic volume V_{ion} and the molar volume V_{mol}. Furthermore, it was found in [11] that for A/N_A and $(V'/V_0)^{3/2} < 15$, A can be expressed as function of V' and the volume at standard conditions through a general relation for oxides:

$$V(P) = N_A V_{ion}(P) \cdot \left[0.61(2) \left(\frac{V'}{V_0} \right)^{\frac{3}{2}} - 1.06(9) \right] - V' \tag{3}$$

where V_{ion} is given in $Å^3$ and V_{mol} in cm^3/mol and N_A is the Avogadro number. Relation (3) holds for simple oxides, silicates, and alumosilicates, including rather large structures like garnets, tourmaline, and sodalite, and also for the few cases of borates and titanates where data over extended ranges of pressures were available [11]. Relation (3) appears to be valid also for large framework structures such as zeolites and metalorganic frameworks where $(V'/V_0)^{3/2} < 15$ but with a different constant offset [11]. Relations (2) and (3) held for a large set of simple and complex oxides at pressures above 2 GPa, whereas at lower pressures, directional variations of bond strength caused minor deviations from (2) for most of the examined materials [11]. Temperature is not an explicit parameter in (3) but enters through V'(T) and it is noted that the term $0.61(2) \cdot (V'/V_0)^{3/2}$ is equivalent to the isobar of an ideal phonon Bose gas const$\cdot T^{3/2} = V$, which implies $V' = f(T/\Theta_D)$ (where Θ_D the Debye temperature).

With relations (2) and (3), even a limited set of molar volumes at a given P and T allows for assessing A and V' and thereby for obtaining a robust interpolation of isotherms. Based on (1) and (2), any change in bond coordination or valence of the constituent ions in

a material becomes apparent because the ionic volumes are markedly dependent on bond coordination and valence [12].

In order to test the extension of Relations (2) and (3) to glasses and melts, experimental compression data on silica and germania glasses [1–9], silicate glasses [10,15], and melts [16] are correlated with ionic volumes as defined in Equation (1). Volumetric data that cover large ranges of compression with small pressure increments are given preference here. Given the significant evolution of the methodology of density measurements for amorphous materials at very high pressures, preference has been given to the most recent experimental studies. Ionic volumes are computed based on Equation (2) with pressure-dependent crystal radii from [12] and based on reported bond coordinations. Coordination is given as Roman numbers in superscript, whereas needed valence is given as Arabic numbers in superscript.

3. Results

Figure 1 shows the molar volume of vitreous silica at 300 K between 10 and 130 GPa plotted against the ionic volume of tetrahedrally coordinated Si^{4+} and two-fold coordinated O^{2-}: $V_{ion} = 4/3\pi \left[r(Si^{4+,IV})^3 + 2r(O^{-2,II})^3 \right]$. For volumes between 25 and 34 cm^3/mol, the correlation is linear and the same holds for volumes that are smaller than 21 cm^3/mol. For volumes intermediate between 21 and 25 cm^3/mol, there is significant scatter. Further, it can be seen that the slope of the linear correlation between V_{ion} and V_{mol} for values 25 $cm^3/mol \leq V_{mol} \leq 34$ cm^3/mol is larger than that for molar volumes below 21 cm^3/mol. These two distinct regimes of compression and the intermediate regime of volumes $21 < V_{mol} < 25$ (in cm^3/mol) match the regimes of the four- and six-fold coordination, and of the intermediate coordination of Si that were reported in independent studies and with different experimental methods [1–6]. Thus, the comparison of molar and ionic volume clearly discriminates coordination changes in amorphous silica as well as the range of the transitory regime between 25 and 21 cm^3/mol.
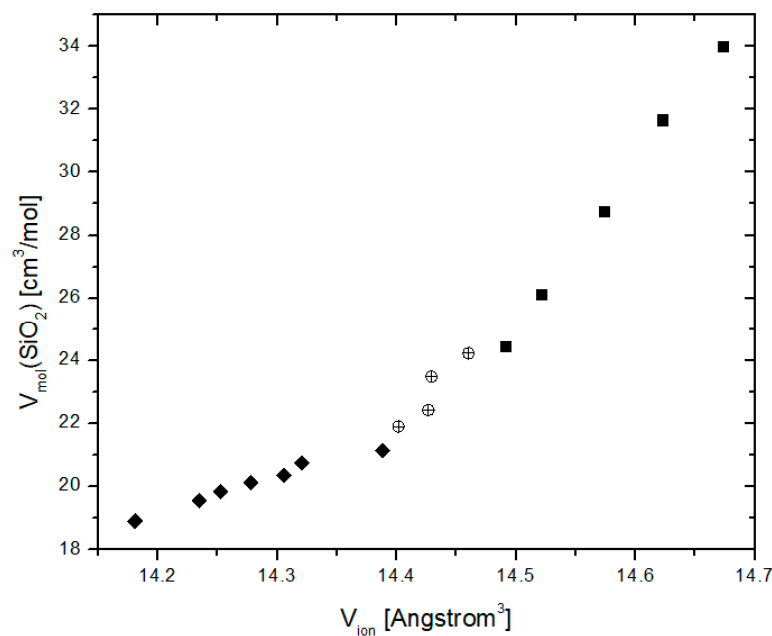

Figure 1. Correlation between ionic and molar volume of compressed vitreous silica at 300 K. The molar volumes are taken from [1]. The ionic volumes are calculated for fixed coordinations Si^{IV} and OII for reference (see below). Three compression regimes are distinguished: (**a**) linear V_{ion}-V_{mol} relation down to ~25 cm^3/mol (filled squares), (**b**) linear V_{ion}-V_{mol} below 21 cm^3/mol (filled diamonds), and (**c**) an intermediate regime of positive V_{ion}-V_{mol} (hollow circles).

In Figure 1, the coordination change is apparent through a change in the linear slope of the correlation between molar and ionic volume. However, the computed ionic volume in Figure 1 is that of low coordination for both Si and O. Hence, it has to be asked how these correlations change if more appropriate bond coordinations are used for calculating the ionic volumes at high pressure. This is shown in Figure 2 with filled square symbols. The data that are labeled $Si^{IV}O_2$ give the same correlation V_{ion}-V_{mol} as in Figure 1 for volumes between 25 and 34 cm^3/mol. However, the data labeled as $Si^{VI}O_2$ are the molar volumes ≤ 21 cm^3/mol which are plotted now against ionic volumes $V_{ion} = 4/3$ $\pi[r(Si^{4+,VI})^3 + 2r(O^{-2,III})^3]$. Hollow and half-filled symbols show equivalent correlations for several crystalline polymorphs of silica taken from [11] for comparison.
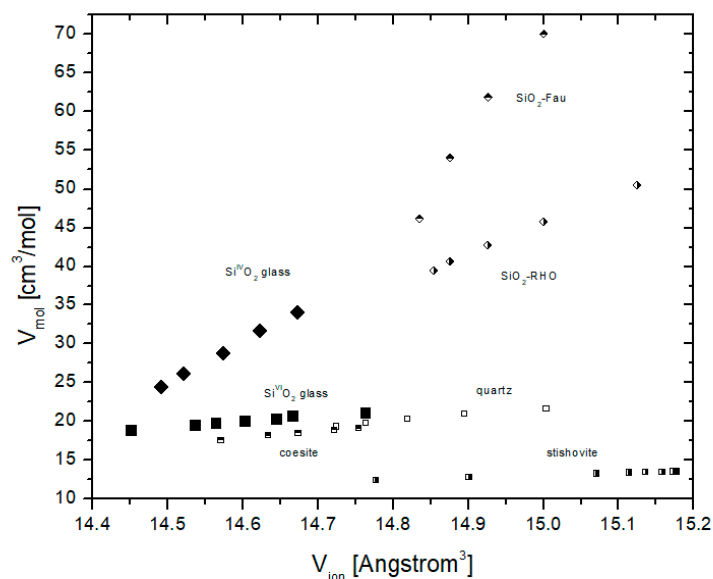

Figure 2. Correlation of pressure-dependent ionic and molar volumes of silica. Filled symbols: vitreous silica; hollow and half-filled symbols: crystalline polymorphs of silica. Ionic volumes are calculated based on Equation (2) for the proper bond coordinations. Molar volumes of vitreous silica are from [1]; the data for the crystalline polymorphs are taken from [11]. 'Fau' and 'RHO' stand for the faujasite- and 'rho'-type zeolite silica frameworks.

Once more, the correlations are linear with a very high degree of correlation (with R^2 0.97 and 0.98). Because the crystal radius of Si^{VI} is larger than that of Si^{IV} while the contraction from O^{II} to O^{III} is rather small [14], the ionic volumes for silica with these different coordinations overlap and the same holds for the ionic volumes for the different crystalline polymorphs that are also shown. This reflects the fact that by definition crystal ionic volumes abstract from any sterical configuration of atoms. However, it is obvious that the slopes for high- and for low-density polymorphs differ, where the linear relations of V_{ion}-V_{mol} for low-density polymorphs are generally steeper than those for high-density polymorphs.

Thus, Figure 2 confirms linearity in the V_{ion}-V_{mol} relations for the coordinations that have been proposed for this range of compression in the experimental studies [1–6]. It is noteworthy that the V_{ion}-V_{mol} relation for fused quartz (low-density vitreous silica) is steeper than that of quartz but similar to that of a small framework structure like RHO (a small-framework zeolite; RHO from 'rhombohedral'). This is remarkable because fused quartz lacks the comparatively much larger voids of the RHO framework structure. The similarity in the compression of low-density vitreous silica and small framework silica polymorphs such as RHO indicates a similarity not in structure but in compression itself and reflects a flexibility of rearranging structural units upon the compression of the vitreous material larger than that of crystalline quartz but similar to that of more open silica network structures.

As indicated, increasing cation coordination at fixed formal valence implies larger ionic volumes and this causes ionic volumes of dense phases to match ionic volumes of low-coordinated polymorphs at a low density. However, the correlations of these ionic volumes with the actual molar volumes are different and so are the slopes of the linear correlations between molar and ionic volumes of different coordination. These two facts suggest that one can define corresponding states based on these slopes and the ionic volumes. This is, in principle, achieved through Equation (3).

As mentioned in the introduction, the slope A of Equation (2) has been found to be similar for isotypic solids, whence one can expect A to be sensitive for bond coordination in non-crystalline materials. Accordingly, Figure 3 shows the slopes A of the molar–ionic volume correlations plotted versus the ratio of the material specific V' and $V_0 = V$ at ambient conditions for all non-crystalline materials that are discussed here, in their high- and low-density regimes (black diamonds) along with the data for crystalline materials taken from [11].
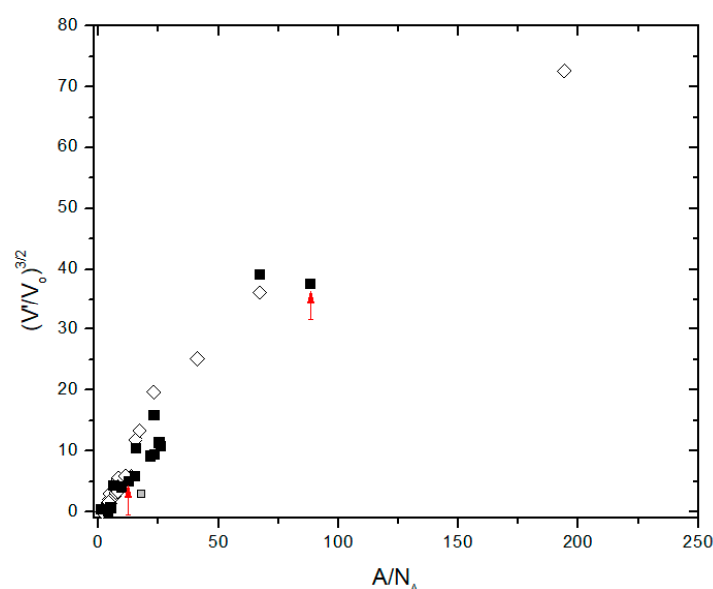

Figure 3. Relation between the slope A of the V_{ion}-V_{mol} correlations for vitreous and crystalline materials; black squares: vitreous materials; hollow diamonds: crystalline phases. The relation between A and $(V'/V_0)^{3/2}$ is based on Equation (3) that was derived in [11]. The data for crystalline phases are taken from [11]. The data for vitreous materials are from this paper using molar volumes from refs. [1,2,6,7,9,10,15,16]. Gray squares represent tests for the correlation between A and the bond coordination: they give A and V' for high-density vitreous silica but with intentionally chosen incorrect coordination IV and II for Si and O (see lines 191–200). Red arrows points to the corresponding values of A and V' for the proper coordinations VI and III for dense and IV and II for low-density vitreous silica with $A/N_A = 12.3$, $(V'/V_0)^{3/2} = 5.10$) and $A/N_A = 88.0$, $(V'/V_0)^{3/2} = 37.7$, respectively. This shows that the relation between A and $(V'/V_0)^{3/2}$ is sensitive to bond coordination. Thus, wrong coordination gives values that are distinctly off the general relation.

In Figure 3, high- and low-density vitreous silica are indicated by red arrows. First, it can be noticed that the two vitreous silica phases do not deviate from the general trend that is defined by the $A \propto V'/V_0$ relation for both crystalline and non-crystalline materials. Secondly, the data for high-density vitreous silica plots very close to the those of stishovite whereas low density vitreous silica plots into the range of small framework structures like RHO-A [11] but markedly above quartz. This is clear from Figure 2 already.

A test of the discrimination of bond coordination can be made by using Equation (3) and comparing the slopes A obtained for trial coordinations with the general trend in the correlation between A and V'/V_0. In Figure 3, the slope A and V' of the correlation of high-density vitreous silica and the ionic volume of Si^{IV} and O^{II} is shown as grey square. A

red arrow points to the value that is obtained for Si^{VI} and O^{III}. The data point (grey square) falls significantly off the general trend in Figure 3 but V_{ion} for Si^{VI} and O^{III} gives A and V' that plot right onto the general trend. Hence, Equation (3) provides constraints even for unknown bond coordination although the correlation exhibits some scatter, as to be expected for a relation that correlates many different structures, compositions, and bond coordinations (Figure 3). A more rigorous assessment of bond coordination is discussed below for $MgSiO_3$.

These findings are now briefly extended to other materials. The results for vitreous germania are shown in Figure 4a,b. For GeO_2, the correlation between molar and ionic volumes is as discriminative as it is for silica. The same holds for vitreous $MgSiO_3$ (Figure 5a,b). Finally, available data of melt compression (melted jadeite, $NaAlSi_2O_6$ [16]) are shown in Figure 6.

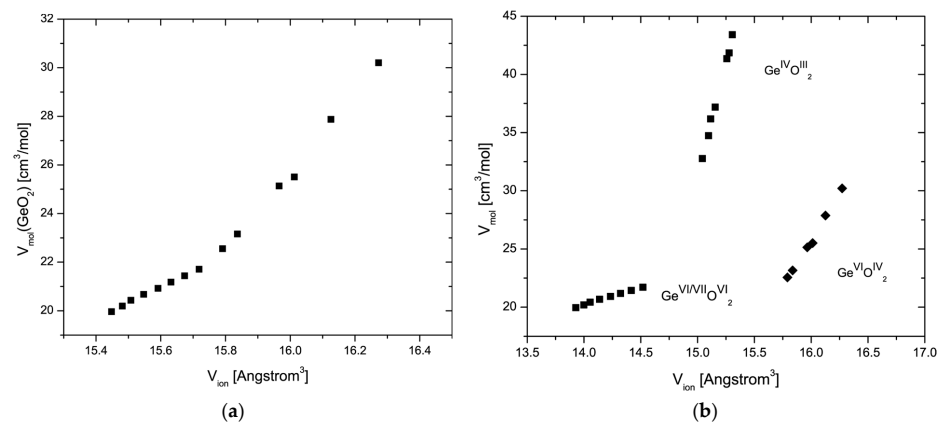**Figure 4.** Relation of ionic and molar volume for vitreous GeO_2. (**a**): V_{ion} with fixed coordination, indicating the relative change in the V_{ion}-V_{mol} relation and the regimes of linearity of different actual bond coordinations. (**b**): V_{ion}-V_{mol} for the experimentally proposed bond coordinations. Molar volumes were taken from [7–9], and pressure-dependent ionic volumes based on Equation (2) with pressure-dependent radii from [12]. Ge^{VI} and Ge^{VII} in dense vitreous germania are not discriminable through the relation.
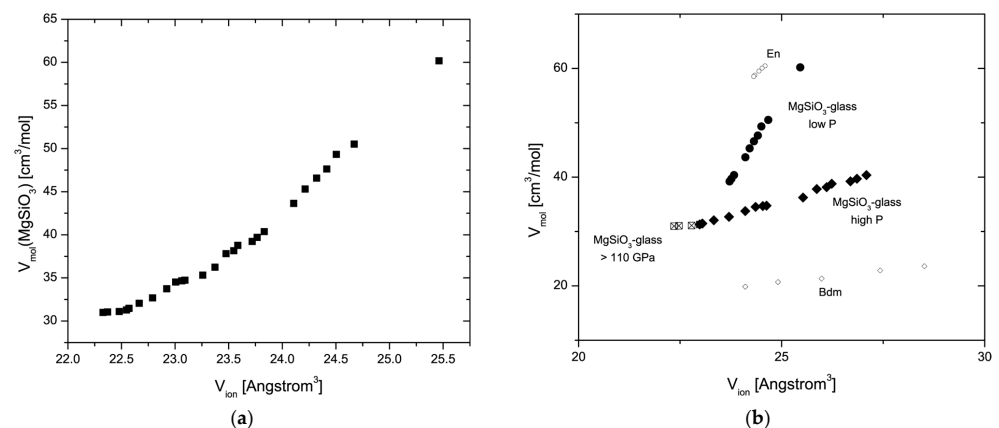

Figure 5. Relation of ionic and molar volume for vitreous $MgSiO_3$. (**a**): V_{ion} with fixed coordination Mg^{VI}, Si^{IV}, O^{II}, indicating the relative change in the V_{ion}-V_{mol} relation and the regimes of linearity of different actual bond coordinations. (**b**): V_{ion}-V_{mol} for the experimentally proposed bond coordinations. The relations for enstatite and bridgmanite are shown for reference. As in the case of silica, vitrous $MgSiO_3$ is generally more compressible than crystalline reference phases. The actual coordination of the vitreous phases in the low- and high-pressure regime are described in the Section 4. Molar volumes were taken from [10], pressure-dependent ionic volumes based on Equation (2) with pressure-dependent radii from [12]. V_{ion}-V_{mol} relations of bridgmanite and enstatite were taken from [11].
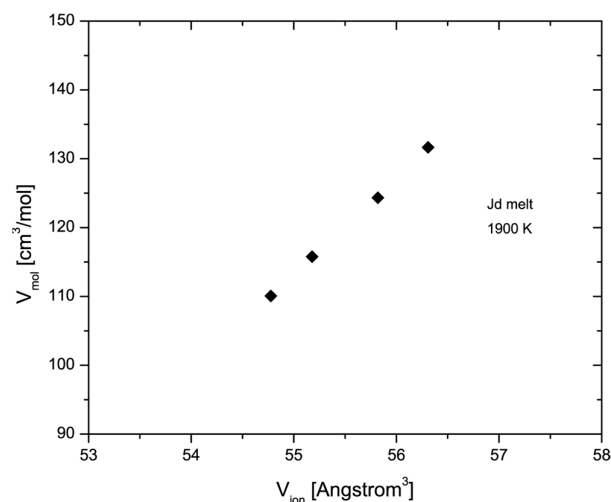
Figure 6. Relation of ionic and molar volume for molten $NaAlSi_2O_6$. V_{ion} was calculated for Na^{VI}, Al^{VI}, Si^{IV}, and O^{III}. The relation is linear, and consistent with rather constant bond coordinations over this range of isothermal volumes. Molar volumes of molten $NaAlSi_2O_6$ are taken from [16]; ionic volumes calculated with Equation (2) are based on pressure-dependent crystal radii from [12].

For these glasses and melts too, the molar–ionic volume correlations fall onto the general trend that is defined by Equation (3). For germania, the transitions between four- and six-fold coordinated Ge^{4+} and the transitory regime with possible five-fold coordinated Ge [7] or the coexistence of coordination are clearly visible in Figure 4a. Equivalent to silica, the molar–ionic volume correlations of germania and $MgSiO_3$ reproduce the coordination that was experimentally assessed; their A- and V′-values plot onto the general correlation shown in Figure 3.

4. Discussion

The results show that the strong linear relation between molar and ionic volumes extends from crystalline phases to glasses and melts with O as a constituent anion. This linear relation implies that the compression of non-crystalline oxides is controlled by the contraction of the spherical average of the valence electron distribution rather than by sterical effects and specific directional bonds, same as that of crystalline solids. This statement does not suggest that the ionic model represents the actual chemical bonds in these materials. However, pressure-dependent interatomic distances are reproduced by the pressure-dependent crystal radii of appropriate coordination. This statement holds for crystalline oxides [11] and we show below that it also holds for non-crystalline oxides with covalent bonds, at least for Mg-silicate. The linear relation between molar and ionic volumes is a sensitive probe of coordination changes in amorphous materials as shown in Figures 1, 4a, 5a, and 6. The available data show that upon compression glasses and melts remain within uncertainties in states of stable cat- and anion coordination rather than exhibiting gradual changes over the whole range of compression. Between those regimes of rather constant bond coordination, transition regions of changing coordination are observed (Figures 1 and 4–6). Within experimental uncertainties, these regimes of noticeably changing bond coordination are limited in comparison to the total compression range and this is in agreement with the earlier findings that conventional equation-of-state fits well represent distinct regimes of glass compression [1–10]. The V_{ion}-V_{mol} relation is, therefore, a strong diagnostic tool for assessing coordination changes in non-crystalline materials. Actual bond coordination is assessed through (a) the slope of the V_{ion}-V_{mol} relation (Figure 3) and (b) observed interatomic distances. This latter point is now discussed in more detail.

Figure 7 shows as filled squares the interatomic distances Si-O and Mg-O of compressed vitreous $MgSiO_3$ between 8 and 126 GPa that were obtained from comparing

experimental inelastic X-ray scattering data of compressed $MgSiO_3$ with molecular dynamics calculations of glass structures and spectra [15]. The hollow symbols are Si-O and Mg-O distances obtained here from pressure-dependent crystal radii [12]. Overall, the pressure-dependent radii reproduce the distances from [15] very well and reproduce the compression-induced changes in bond coordination. The regimes of bond coordination are indicated in Figure 7. Agreement between both sets of data is optimal in the 20 to ~80 GPa range and exhibits positive deviation at higher pressure, which suggests that the coordination of Mg and Si increased and crystal radii, which were used here, were therefore somewhat overestimated; that is, the ions have higher bond coordination than assumed. Generally, the bond coordination of O is higher in the crystal-radii based assessment than proposed by Kim et al. [15]. It is plausible that the inelastic X-ray scattering (IXS) spectra from the O k-edge [15] emphasize transitions of O s- and p-electrons whereas the crystal radii also account for spherically averaged d-states, which at pressures in excess of 50–100 GPa are involved in the valence states of O. Thus, it is plausible that the crystal radii represent in part different valence states than what IXS probes. In particular, it is noted that the best match of distances above ~50 GPa was obtained with crystal radii of O^{IV}, which differs from the assessment of O-coordination in [15] but agrees with the assessment of O-coordination on silica in the 100 GPa range [2].
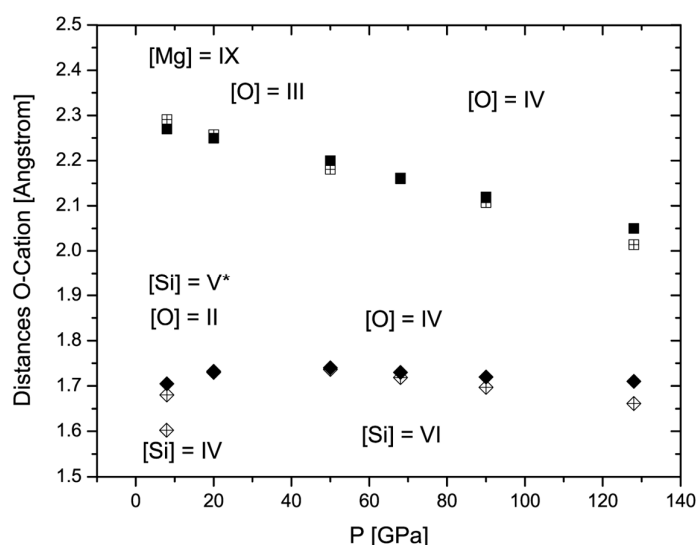

Figure 7. Interatomic cation–anion distances in compressed vitreous $MgSiO_3$. Black diamonds: Data from Kim et al. [15]. Hollow diamonds: Calculated based on pressure-dependent crystal radii [12]. The bond coordinations that were used for the crystal radii are shown. The change in bond coordination in the compressed glass is reproduced by the crystal radii model.

In any case, the overall agreement is quite good. The Si-O value for Si^{IV} at 8 GPa is given for reference and is markedly shorter than the one reported in [15]. It is noted that the assessment of distances in [15] is not purely empirical. However, the agreement between the values reported in [15] and here proposes that distances obtained from pressure-dependent crystal radii could well serve as input in the analysis of pair distribution functions from total scattering data for the fully experimental assessment of interatomic distances in non-crystalline materials, even at high pressures in excess of 100 GPa.

Only one set of volumetric data for a silicate melt is available ([16], Figure 6). As in the case of glasses, this melt shows stable bond coordination over the examined range of compression. Volumetric studies of oxide (and silicate) melts are difficult at combined high temperature and pressure. Hence, a plain practical advantage of the linear molar–ionic volume Relation (2) is in the assessment of isotherms different from 300 K where a few data points suffice for assessing the relation and thereby the isothermal compression. A more explicit treatment of the thermal effects through the parameter $V' = f(T/\Theta_D)$ has the

potential of reducing the overall scatter of the general Relation (3) and may render this relation more precise in assessing bond coordinations in non-crystalline materials.

5. Conclusions

A linear relation between crystal ionic and empirical molar volumes is shown to hold for oxide-based non-crystalline materials, including silicates. This finding extends earlier work on crystalline oxides and halides. For non-crystalline materials, the newly established relation provides a strong diagnostic tool for finding regimes of constant or nearly constant bond coordination in glasses and melts. Moreover, it is shown here that the transitory regimes of irreversed changes in coordination are not gradual over the entire range of compression but rather limited to pressure ranges much smaller than the regimes of constant coordination of the same material. Pressure-dependent crystal radii allow for the prediction of average bond coordinations and interatomic distances which are a useful input in pair distribution function analyses of amorphous scattering data.

Data Availability Statement: All discussed data and results are shown in the figures of this paper. Data from earlier work are referenced throughout.

Conflicts of Interest: The author declares no conflicts of interest.

References

1. Petitgirard, S.; Malfait, W.J.; Journaux, B.; Collings, I.E.; Jennings, E.S.; Blanchard, I.; Kantor, I.; Kurnosov, A.; Cotte, M.; Dane, T.; et al. SiO$_2$ Glass Density to Lower-Mantle Pressures. *Phys. Rev. Lett.* **2017**, *119*, 215701. [CrossRef] [PubMed]
2. Lee, S.K.; Kim, Y.H.; Yi, Y.S.; Chow, P.; Xiao, Y.M.; Ji, C.; Shen, G.Y. Oxygen Quadclusters in SiO$_2$ Glass above Megabar Pressures up to 160 GPa Revealed by X-ray Raman Scattering. *Phys. Rev. Lett.* **2019**, *123*, 235701. [CrossRef] [PubMed]
3. Murakami, M.; Kohara, S.; Kitamura, N.; Akola, J.; Inoue, H.; Hirata, A.; Hiraoka, Y.; Onodera, Y.; Obayashi, I.; Kalikka, J. Ultrahigh-pressure form of SiO$_2$ glass with dense pyrite-type crystalline homology. *Phys. Rev. B* **2019**, *99*, 045153. [CrossRef]
4. Kono, Y.; Shu, Y.; Kenney-Benson, C.; Wang, Y.B.; Shen, G.Y. Structural Evolution of SiO$_2$ Glass with Si Coordination Number Greater than 6. *Phys. Rev. Lett.* **2020**, *125*, 205701. [CrossRef] [PubMed]
5. Kuang, H.Y.; Sahle, C.J.; Petitgirard, S.; Tse, J.S. Correlation of the structures of dense silica with X-ray Raman spectra. *Phys. Rev. B* **2024**, *109*, 054110. [CrossRef]
6. Lobanov, S.S.; Speziale, S.; Winkler, B.; Milman, V.; Refson, K.; Schifferle, L. Electronic, Structural, and Mechanical Properties of SiO$_2$ Glass at High Pressure Inferred from its Refractive Index. *Phys. Rev. Lett.* **2022**, *128*, 077403. [CrossRef] [PubMed]
7. Petitgirard, S.; Spiekermann, G.; Glazyrin, K.; Garrevoet, J.; Murakami, M. Density of amorphous GeO$_2$ to 133 GPa with possible pyritelike structure and stiffness at high pressure. *Phys. Rev. B* **2019**, *100*, 214104. [CrossRef]
8. Kim, Y.H.; Yi, Y.S.; Kim, H.I.; Chow, P.; Xiao, Y.M.; Shen, G.Y.; Lee, S.K. Pressure-Driven Changes in the Electronic Bonding Environment of GeO$_2$ Glass above Megabar Pressures. *J. Am. Chem. Soc.* **2020**, *144*, 10025–10033. [CrossRef] [PubMed]
9. Hong, X.G.; Newville, M.; Ding, Y. Local structural investigation of non-crystalline materials at high pressure: The case of GeO$_2$ glass. *J. Phys. Cond. Mat.* **2023**, *35*, 164001. [CrossRef] [PubMed]
10. Petitgirard, S.; Malfait, W.J.; Sinmyo, R.; Kupenko, I.; Hennet, L.; Harries, D.; Dane, T.; Burghammer, M.; Rubie, D.C. Fate of MgSiO$_3$ melts at core-mantle boundary conditions. *Proc. Nat. Acad. Sci. USA* **2015**, *112*, 14186–14190. [CrossRef] [PubMed]
11. Tschauner, O. Systematics of Crystalline Oxide and Framework Compression. *Crystals* **2024**, *14*, 140. [CrossRef]
12. Tschauner, O. Pressure-Dependent Crystal Radii. *Solids* **2023**, *4*, 235–253. [CrossRef]
13. Lee, S.K.; Mun, K.Y.; Kim, Y.H.; Lhee, J.; Okuchi, T.; Lin, J.F. Degree of Permanent Densification in Oxide Glasses upon Extreme Compression up to 24 GPa at Room Temperature. *J. Phys. Chem. Lett.* **2020**, *11*, 2917–2924. [CrossRef] [PubMed]
14. Shannon, R.D. Revised effective ionic-radii and systematic studies of interatomic distances in halides and chalcogenides. *Acta Cryst. A* **1976**, *32*, 751–767. [CrossRef]
15. Kim, Y.-H.; Yi, Y.S.; Kim, H.-I.; Chow, P.; Xiao, Y.; Shen, G.; Lee, S.K. Structural transitions in MgSiO$_3$ glasses and melts at the core-mantle boundary observed via inelastic X-ray scattering. *Geophys. Res. Lett.* **2019**, *46*, 756–764. [CrossRef]
16. Xu, M.; Jing, Z.; Van Orman, J.; Yu, T.; Wang, Y.B. Density of NaAlSi$_2$O$_6$ Melt at High Pressure and Temperature Measured by in-situ X-ray Microtomography. *Minerals* **2020**, *10*, 161. [CrossRef]